EquipeDyva/ JournalClub

Program

- **Each Wednesday, from 14:30 to 15:30**, Salle George Morin

SESSION: The good, the bad and THE NOISE

- 04/11 AnnaMontagnini : article *Evaluation of objective uncertainty in the visual system. Simon Barthelme & Pascal Mamassian*
- 11/11 Fete nationale
- 18/11 Amar On the topic: kalman filter : *The statistical determinants of adaption rate in human reaching*
- 25/11 ClaudioSimoncini: Reliability, synchrony and noise, Ermentrout et al. (2006) - Noise can be good: when increasing variability in the sensory input helps (or does not help) motion processing. see also http://en.wikipedia.org/wiki/Stochastic_resonance
- 03/12 (9.30 AM) Adrian Ponce (exceptional seminar) *Dynamic sequence of states in five cortical areas during a discrimination task*
- 09/12 LaurentPerrinet: starting with Mechanisms of visual motion detection, towards *Frozen noise in the icicle model*
- ??/?? Fredo ?? : review Noise in the nervous system. Faisal, Selen and Wolpert, Nat Rev Neurosci 2008

Mechanisms of visual motion detection

Paul R. Schrater[1], David C. Knill[2] and Eero P. Simoncelli[3]

[1] *Department of Psychology, University of Minnesota, N218 Elliott Hall, 75 E. River Dr., Minneapolis, Minnesota 55455, USA*

[2] *Department of Psychology, University of Pennsylvania, 3815 Walnut St., Philadelphia, Pennsylvania 19104, USA*

[3] *Center for Neural Science, New York University, 4 Washington Place, New York, New York 10003, USA*

Correspondence should be addressed to P.R.S. (schrater@eye.psych.umn.edu)

Visual motion is processed by neurons in primary visual cortex that are sensitive to spatial orientation and speed. Many models of local velocity computation are based on a second stage that pools the outputs of first-stage neurons selective for different orientations, but the nature of this pooling remains controversial. In a human psychophysical detection experiment, we found near-perfect summation of image energy when it was distributed uniformly across all orientations, but poor summation when it was concentrated in specific orientation bands. The data are consistent with a model that integrates uniformly over all orientations, even when this strategy is sub-optimal.

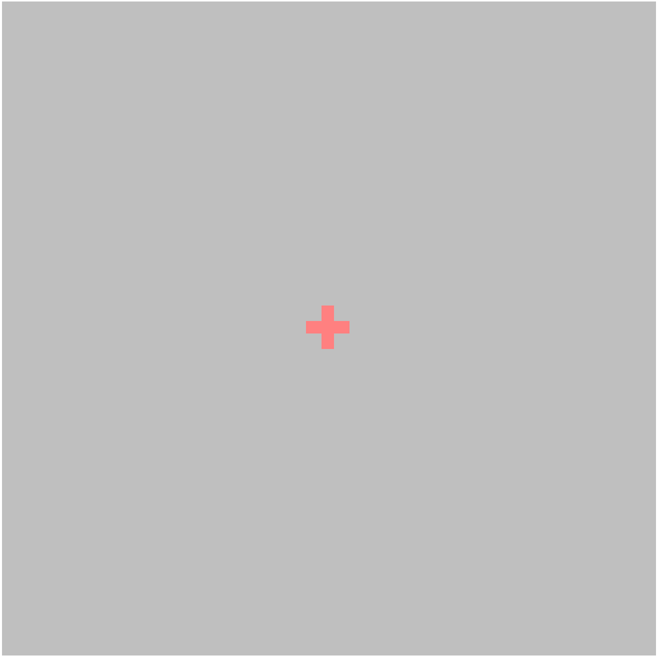

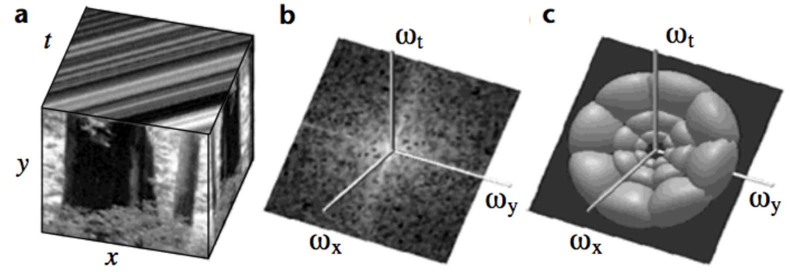

Fig. 1. A translational motion detector. (**a**) Space-time luminance pattern of an image translating to the right. This is a representation of the intensity information in the retinal image (the *x*–*y* plane) over time (*t*). The rightward motion can be inferred from the oriented pattern on the *x*–*t* face. (**b**) The Fourier amplitude spectrum of the luminance pattern, represented by the intensity of points in a three-dimensional spatiotemporal frequency domain. Non-zero Fourier amplitudes are constrained to lie on a plane through the origin. The orientation of this plane uniquely specifies the direction and speed of translation. (**c**) Construction of a translation detector[10], illustrated in the Fourier domain. Pairs of balls symmetric about the origin indicate the Fourier amplitude spectra of band-pass filters whose peak frequencies lie in the plane. A translation detector can be constructed by summing the squared outputs of such filters.

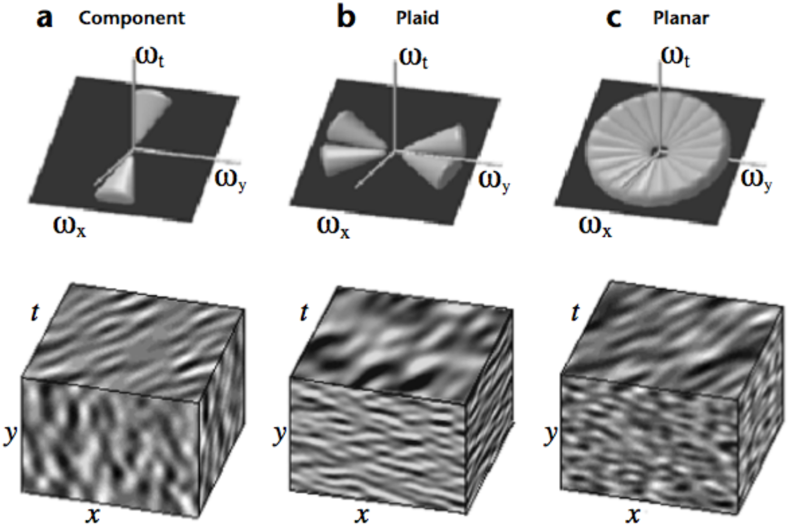
a Component
b Plaid
c Planar
ω_t
ω_y
ω_x
t
y
x

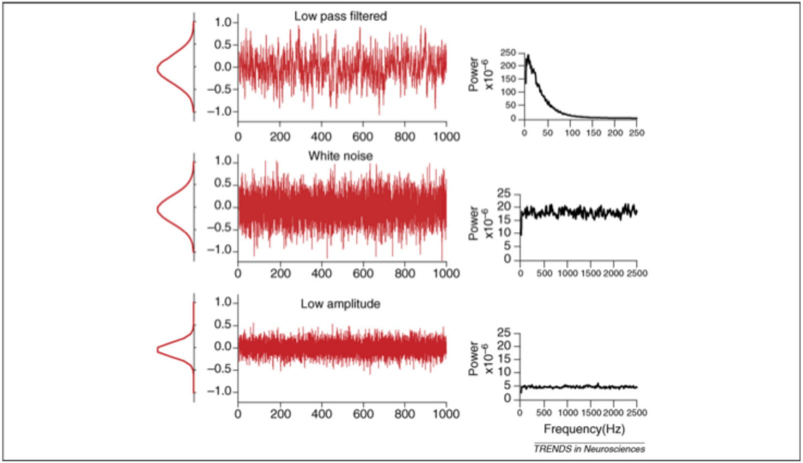

Figure 1. Definition and properties of noise. Graphs show properties of three different noise signals. Middle row of graphs shows Gaussian white noise. That is, the value at each time point is randomly drawn from a Gaussian distribution (shown on far left). Power spectrum shows that the signal contains equal amounts of power at all frequencies from 0 to 2500 Hz. Top row shows low pass filtered noise. Distribution of signal values (far left) is identical to the white noise case, but values at any time point are correlated with those at other time points, resulting in slower fluctuations and a power spectrum that is reduced at high frequencies. Bottom row shows white noise of a lower amplitude than in the middle graph. Distribution of stimulus values (far left) is narrower than for the middle row, but the power spectrum is flat.

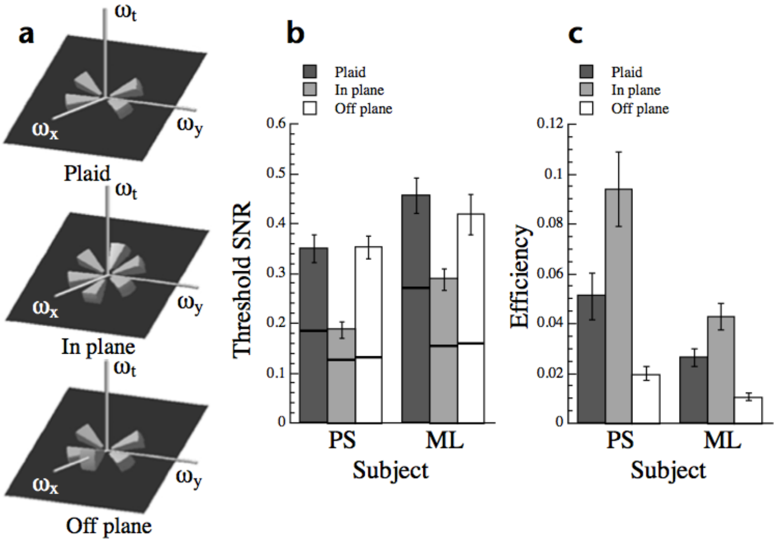

Fig. 4. Experiment 2. (**a**) Filters used to generate stimuli. (**b**) Threshold SNRs for detecting the three types of stimuli in. Black bands indicate the predictions of ideal summation, based on subjects' detection thresholds for the component stimulus used in experiment 1. (**c**) Detection efficiencies for the three stimulus types. The results show a large increase in efficiency for the in-plane triplet over the plaid and a decrease for the off-plane triplet, indicating increased summation with additional power on a common plane.

0: Pink noise enveloppes

0: Pink noise enveloppes

0: Pink noise enveloppes

1: Make it move

1: Make it move

1: Make it move

2: One band

2: One band

2: One band

2: One band (twice)

2: One band (competing)

3: Grating

3: Grating

3: Grating (twice)

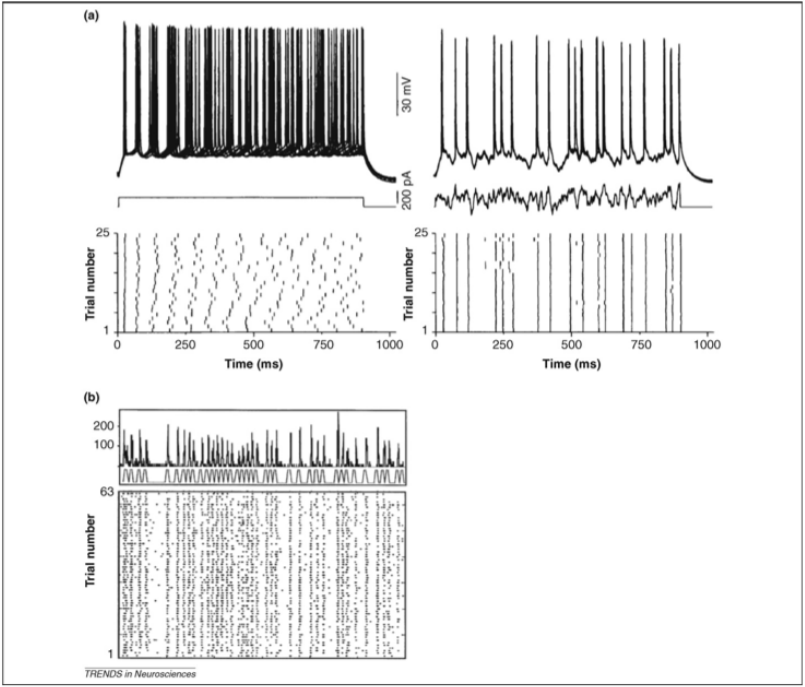

Figure 2. Noisy inputs cause reliable spiking *in vitro* and *in vivo*. **(a)** Left: steady-state current injection into a cortical pyramidal cell *in vitro* results in trains of action potentials shown as voltage traces (top) or spike rasters (bottom). On different trials the first spike is evoked at the same time on each trial, but subsequent spikes are unreliable. Right: injection of fluctuating current causes the cell to spike reliably throughout the spike train. **(b)** *In vivo* recordings from cortical area MT shows reliable

Frozen noise

Frozen noise

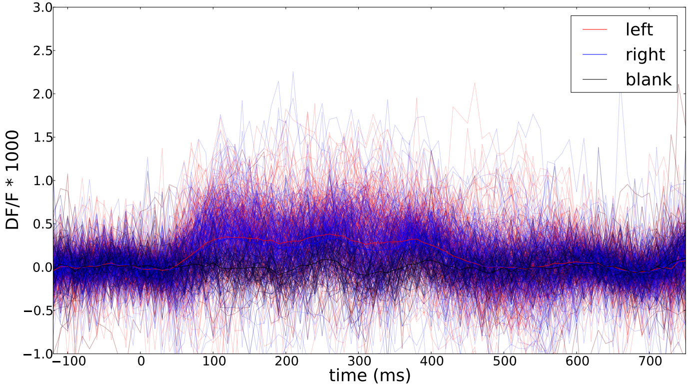

Frozen noise

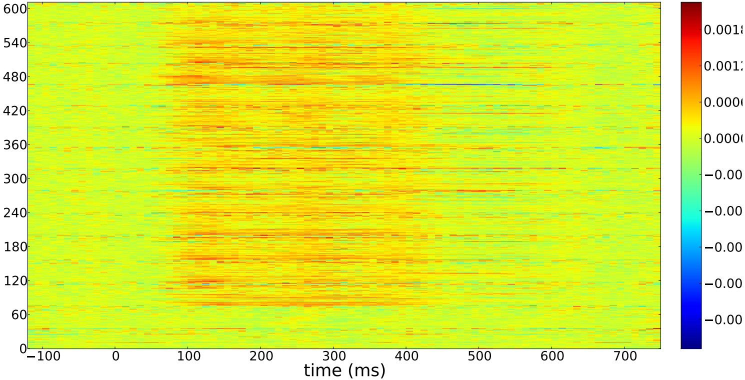

Frozen noise